PROCEEDINGS OF SCIENCE

Studies on Helium flux with DAMPE

Valentina Gallo[1], Paolo Bernardini*[2,3], Peng-Xiong Ma[4], Qiang Yuan[4], on behalf of DAMPE collaboration†

[1] *Département de Physique Nucléaire et Corpusculaire, Université de Genève, Geneva, Switzerland*
[2] *Dipartimento di Matematica e Fisica "E. De Giorgi", Università del Salento, Lecce, Italy*
[3] *Istituto Nazionale di Fisica Nucleare Sezione di Lecce, Lecce, Italy*
[4] *Key Laboratory of Dark Matter and Space Astronomy, Purple Mountain Observatory, Chinese Academy of Sciences, Nanjing 210008, China*

E-mail: valentina.gallo@unige.ch

Since December 2015 the DAMPE (DArk Matter Particle Experiment) detector is on-orbit at an altitude of 500 km and takes data smoothly. It consists of a Plastic Scintillator strip Detector (PSD), a Silicon-Tungsten tracKer-converter (STK), a BGO imaging calorimeter and a NeUtron Detector (NUD). The charge of incident cosmic rays (CRs) is measured by looking at the energy deposited in the PSD, and the tracks are reconstructed thanks to the high spatial resolution of the STK. The remarkable depth (32 radiation lengths) of the calorimeter allows for an estimate of the CR energy. Then the DAMPE features are suitable to distinguish the elemental composition of CRs and to measure their fluxes in the energy range of 20 GeV - 100 TeV. Here the analysis progress in the study of the Helium component will be presented and discussed.

35th International Cosmic Ray Conference — ICRC2017
10–20 July, 2017
Bexco, Busan, Korea

*Speaker.

†The DAMPE mission is funded by the strategic priority science and technology projects in space science of Chinese Academy of Sciences. In China the data analysis is supported in part by the National Key Research and Development Program of China (No. 2016YFA0400200) and the 100 Talents Program of Chinese Academy of Sciences. In Europe the activities and the data analysis are supported by the Swiss National Science Foundation (SNSF), Switzerland, and the National Institute for Nuclear Physics (INFN), Italy.

PoS(ICRC2017)169

1. Introduction

Protons (H) and Helium (He) nuclei are the main components of cosmic rays (CRs), and are believed accelerated by sources as supernova remnants in the Milky Way. Precise measurement of their fluxes as a function of energy can shed light on CR origin, acceleration mechanism and diffusion in the galaxy. Recently several experiments [1, 2, 3, 4, 5] have observed significant He-flux variation at energies of hundreds of GeV. In particular, a single power law does not reproduce these measurements and a clear hardening of the He-flux has been observed. A similar hardening is present also in the proton flux and many models have been proposed to explain this effect. The emerging of CRs from other sources, different acceleration mechanisms and propagation effects have been suggested. The precise measurement of proton and helium fluxes at TeV-energy and beyond is expected to be the crucial check for these hypotheses. Thanks to its high thickness and large acceptance, the DAMPE detector collected CR events in this energy range for more than one year. Here the DAMPE preliminary results about the He flux are presented and compared with those of other experiments.

2. DAMPE detector

The DArk Matter Particle Explorer (DAMPE) [6] is a powerful space detector successfully launched on the 17^{th} December, 2015. The layout of the detector is shown in Fig. 1. It is made of

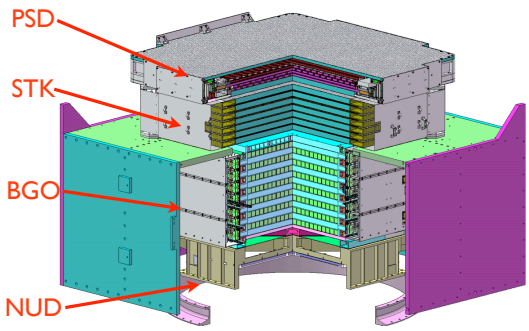

Figure 1: Layout of the DAMPE detector.

the following sub systems: a double layer plastic scintillator strip detector (PSD) [7] used as anti-coincidence for incoming photons and for the measurement of the charge (Z) of incident particles; a silicon-tungsten tracker-converter (STK) [8] dedicated to the reconstruction of the trajectories of charged particles, the photon conversion in electron-positron pairs and the measurement of the particle charge (Z); a bismuth germanium oxide imaging calorimeter (BGO) [9] of about 32 radiation lengths and about 1.6 nuclear length for precise energy measurements and electron/photon identification with respect to hadrons; a neutron detector (NUD) to increase the electron/proton separation power.

3. Data analysis

In this analysis the results obtained since the first year of operation (from the 1^{st} January to the 31^{st} December 2016) are reported. The DAMPE detector was in a stable data taking mode and the number of recoded events was of about 1.8 billions for a mean of 5 millions of events per day as shown in Fig. 2. Small interruptions of the data acquisition are due to the detector maintenance and calibration. The average daily live time of the DAMPE detector is of about

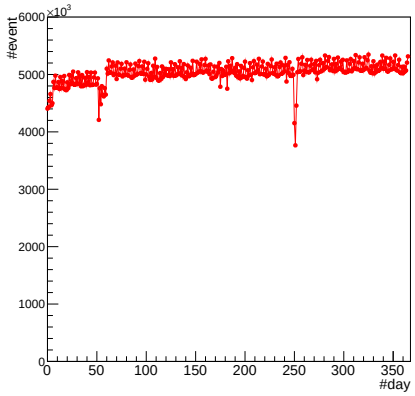

Figure 2: Number of events per day recorded by DAMPE from the the 1^{st} January to the 31^{st} December.

18.4 hours. The detectors are not operating for a mean of 4 hours per day due to the acquisition dead time of 3.0725 ms after each trigger. The satellite crosses the South Atlantic Anomaly (SAA) region on average for 1 hour per day and the related events are excluded from the analysis presented in the following. More details on the evaluation of the SAA can be found here [10]. A residual contribution to the detector dead time is due to the on-orbit calibration procedures of the sub-detectors.

3.1 Event selection

In this analysis only particles releasing an energy in the BGO above 20 GeV are considered in order to remove the effect of the geomagnetic cutoff. Moreover, in order to select only particles crossing all the sub systems and well contained in the BGO volume the following **pre-selection cuts** are applied:

- *BGO Acceptance*: the reconstructed direction of the particle shower in the BGO is projected to the top and to the bottom of the BGO and only events contained within 280 mm from the center are considered.
- *Max Bar cut*: events releasing the maximum energy in the last or first bar of the second, third and forth layer are also rejected.
- *Lateral shower cut:* to exclude particles coming from the side of the detector a cut on the energy shower shape is applied, events with more than 35% of total energy deposited in one layer are rejected.

After the pre-selection cuts, the events in the SAA are removed and only events with at least one reconstructed track in the STK are selected, then to select the right track the following **BGO-STK match cut** is applied. The tracks are chosen if there is at least one hit on the first STK layer, subsequently used to identify the charge (Z) of the incoming particle as discussed in Sec. 3.2. The track direction is than requested to match the direction of the BGO shower: only tracks within 20° from the BGO shower direction and with a track projection on the first BGO layer that does not exceed 60 mm from the BGO shower projection on the same layer are selected. If more than one track passes the selection, the track closer to the BGO shower direction is chosen.

In order to identify the PSD bars crossed by the incoming particle a **STK-PSD match cut** is applied. The track direction is projected on the PSD and only bars within 20 mm from the X and Y view track projections and with an energy above 0.5 MeV are selected. If the projection of the track direction is outside or at the border of the PSD planes the event is rejected.

The number of events as a function of the energy for these selection cuts is shown on the left panel of Fig. 3. About 5% of the total acquired data survives the cuts.

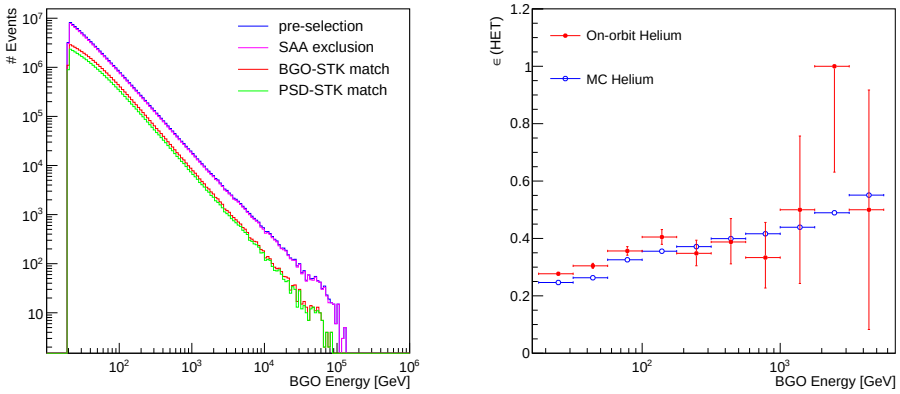

Figure 3: (Left) Number of events as a function of reconstructed BGO energy passing the selection cuts. (Right) High Energy Trigger (HET) efficiency as a function of BGO energy.

On the right panel of Fig. 3, the High Energy Trigger (HET) efficiency is shown as a function of BGO Energy for both data and Monte Carlo (MC), the MC simulation has been performed using the GEANT4 toolkit [11]. The HET efficiency is computed with respect to the unbias trigger that is highly pre-scale as a function of the latitude (1/512 for $|\text{latitude}| \leq 20^\circ$ and 1/2048 elsewhere), that is why the statistics at E > 1 TeV is quite limited. This efficiency is evaluated for both data and MC, the highest observed discrepancy being of 15.8% for BGO Energy below 200 GeV is used as systematic uncertainty.

3.2 Charge reconstruction

A crucial measurement for this analysis is the particle charge reconstruction. As described in the previous section, the charge can be identified using both the PSD and the STK detectors. From hereafter we will refer as PSD charge the $\sqrt{E(MeV)/2}$ where 2 is used as reference since 2 MeV is expected to be the mean energy released by a proton MIP in one PSD bar and E is the PSD

energy after applying the attenuation correction factors described in [12] and taking into account the particle path-length inside the bar. This parameter is not the exact particle charge (Z=2) since the energy loss in the PSD bars results to be depended on the energy of the incoming particle as shown in Fig. 4 where the Most Probable Value (MPV) from a Landau fit of the $\sqrt{E(MeV)/2}$ distributions is shown as a function of the BGO energy. Moreover, the energy loss results to be always higher for the second PSD layer, that is the most internal one.

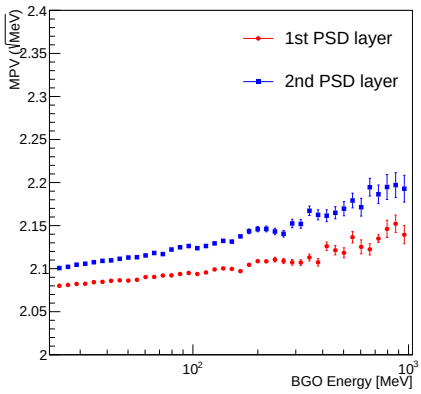

Figure 4: Most Probable Value (MPV) from a Landau fit of the $\sqrt{E(MeV)/2}$ distribution as a function of the BGO energy.

A data MC comparison of the PSD charge distributions for a selected Helium sample in six energy bins and for the first PSD layer is shown in Fig 5. The MC well simulates the Helium energy loss in the PSD and a similar result is also obtained for the second PSD layer.

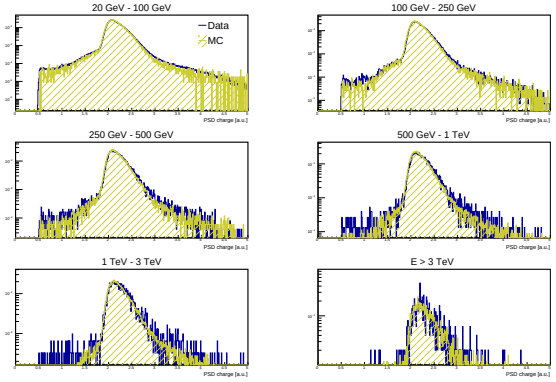

Figure 5: Data (blue line) Monte carlo (yellow area) comparison of the PSD charge in six energy bins for the first layers of the PSD.

In order to reduce the proton contamination an additional cut on the first layer of STK is used. The charge measured in at least one of the first silicon layers (X or Y view) of STK has to be compatible with Helium charge, a description on the charge identification from STK can be found in [13]. This selection allows to have a good Helium identification before the interaction with the

STK tungsten plates. On the left side of Fig. 6 the efficiency of this selection cut is shown as a function of the BGO energy for both data and MC. The STK charge selection efficiency results to be constant as a function of energy and there is a good agreement between data and MC and the associated systematic uncertainty is negligible, that is of the order of few percent.

The charge correlation between the two PSD layers after this cut is shown on the right panel of Fig. 6. Events with a reconstructed PSD charge above 4 in both PSD layers (red dashed line in the figure) are rejected in order to exclude ions with higher Z. Despite the good charge identification

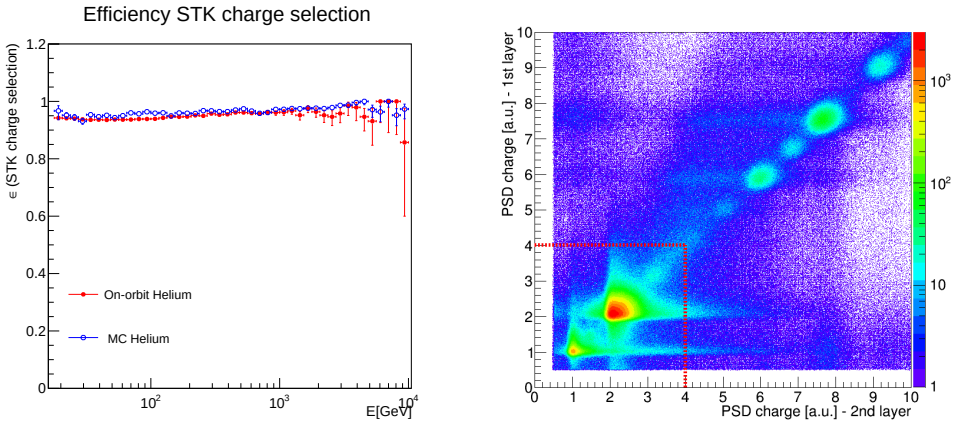

Figure 6: (Left) STK charge selection efficiency for data (blue points) and Helium MC (red points) as a function of BGO energy. (Right) PSD charge correlation between in the two PSD layers for events passing the STK charge selection. The red dashed lines indicate the cut applied to exclude ions with higher Z.

resolution of the PSD, the correlation between the charge reconstructed in the two PSD layers (right panel of Fig. 6) is affected by the interactions of the particles inside the PSD layers and the possible mis-identification of Z in one of the layers, therefore a charge difference between the two layers not greater than 0.8 is required. This cut will help in a better estimation of the proton contamination as shown in the next section.

In the two panels of Fig. 7 the charge identification efficiencies for data and MC and for both PSD layers are shown. Also in this case there is a good agreement between data and MC, with a slight decrease of efficiency for BGO energy above 1 TeV. The highest observed discrepancy for the first and second layer and BGO energy below 1 TeV is respectively of 5% and 7%. For higher energy a higher systematic uncertainties of 7% for the first and 12% for the second PSD layer is observed and evaluated as the maximum difference between data and MC up to 4 TeV.

3.3 Proton contamination

The main background for the Helium selection is due to the protons which are the most abundant particles in the Cosmic Rays. As discussed before, events with a charge difference between the first and second PSD layers greater than 0.8 are excluded to reduce the interactions in the PSD layers which would imply a greater contaminations by protons in the Helium as shown also on the left panel of Fig. 8. The charge difference is defined as $PSD_{diff} = |PSD_2 - PSD_1 - 0.03|$, the offset to the charge being due to the higher energy loss in the second PSD layer, as shown in Fig. 4. The pro-

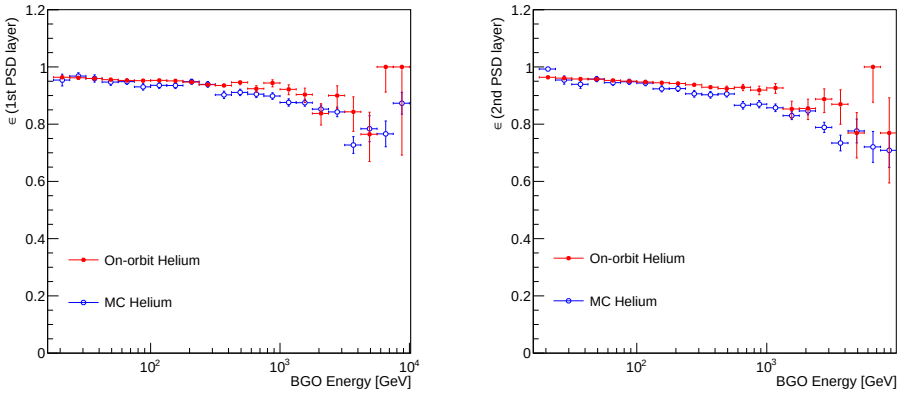

Figure 7: Charge identification efficiency for the first (Left) and second (Right) PSD layer and for both data (red) and MC (blue) as a function of BGO energy.

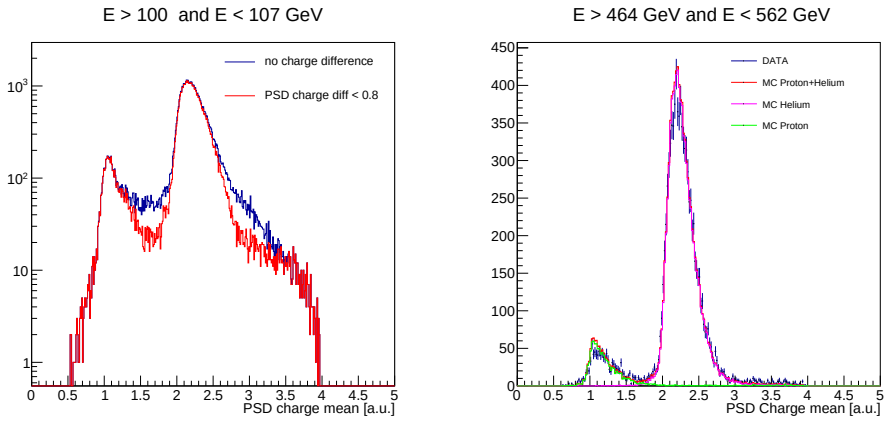

Figure 8: (Left) PSD charge mean in the BGO energy range of 100-107 GeV with and without the PSD charge difference cut of 0.8. (Right) Template fit example for the evaluation of the proton contamination in the Helium selection.

ton contamination is estimated with a template fit of the MC samples to the data of the arithmetic mean of the charge measured in both PSD layers, referred hereafter as PSD charge mean. The fit is performed using the TFractionFitter class of the ROOT framework [14]. As an example, on the right panel of Fig. 8 the resulting fit for one energy bin is shown together with the data, as well as with proton and Helium MC templates. For energy below 400 GeV a small fraction of Lithium is present and taken into account in the fit. A constant and wide cut on the PSD charge mean between 1.8 and 2.8 is applied to select the Helium candidates and it is also shown in the same figure. The proton contamination is estimated to be below the 1% for BGO energy lower than 1 TeV and below 1.5% at higher energy, as shown in Fig. 9.

3.4 Results

At the end of the selection the effective acceptance is around 0.035 m^2 sr for a primary Helium

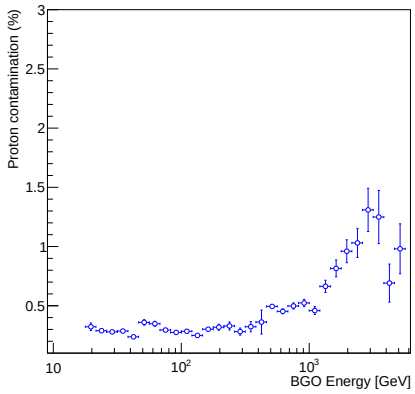

Figure 9: Proton contamination as a function of the BGO energy, the contamination results to be less than 1% for energy below 1 TeV. The overall contamination is below 1.5%.

energy between 100 GeV and 10 TeV, while the proton acceptance in this He-analysis is less than 0.001 m^2 sr, as shown on the left side of Fig 10 and the proton contamination for the Helium sample results to be negligible. The effective acceptance is based purely on the MC and is defined as:

$$A_{eff,i} = A_{gen} \times \frac{N_{pass,i}}{N_{gen,i}}$$

where A_{gen} is the geometrical term due to the MC particle generation on half spere surrounding the detector, $N_{pass,i}$ is the number of events passing all the Helium selection cuts in a given primary energy bin i and $N_{gen,i}$ is the corresponding number of events generated in the same energy bin. A very preliminary measurement of the flux of Helium nuclei as a function of nucleon kinetic energy is shown on the right panel of Fig. 10, where the DAMPE points are shown in black and are compered with the AMS-02 [1], CREAM [4] and PAMELA [5] measurements. An unfolding method based on [15, 16, 17] was used to estimate the Helium candidates energy. So far the uncertainty on the unfolding method is not taken into account as well as the energy resolution for Helium. The shadow area in the plot describes the very preliminary systematic uncertainty of 21% of the effective acceptance that has been evaluated as the sum in quadrature of the maximum values of systematic uncertainties of the HET and PSD charge selection efficiencies previously described. The evaluation of the systematic uncertainties is not yet conclusive, further studies are in progress to get a more exhaustive and bin-by-bin evaluation of the systematic uncertainties.

4. Conclusion

Although the Helium flux measurement reported here is very preliminary, this result by DAMPE is in a good agreement with the previous experiments and with an indication of a hardening of the Helium flux as also reported by other experiments. After only one year of data taking the number of Helium candidates with a reconstructed BGO energy above 10 TeV is of about 150 events which correspond to already few tens of candidates with an energy of about 100 TeV, as from preliminary MC estimation. In the next future with the increasing of the data collection and improving of

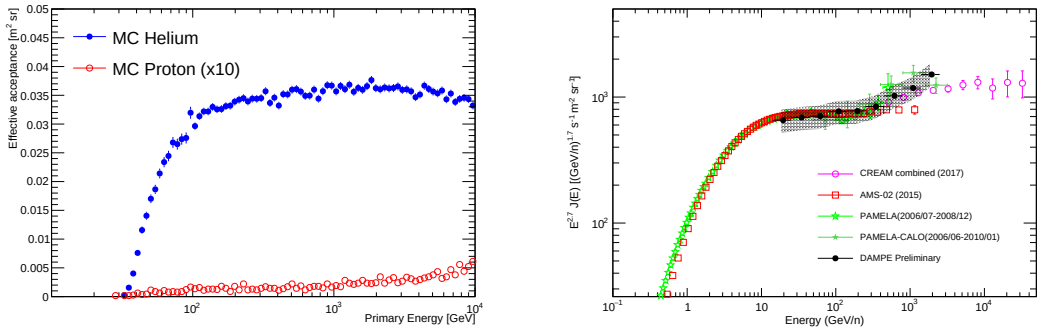

Figure 10: (Left) Effective acceptance for the proton and Helium MC samples after the cut selection. (Right) Helium flux times $E^{2.7}$ as a function of primary energy.

the analysis procedures DAMPE is expected to provide measurements of the Cosmic Rays spectrum up to 100 TeV particle energy, this will contribute to a better understanding of the origin and propagation mechanism of high energy Cosmic Rays.

References

[1] M. Aguilar et al. (AMS Collaboration), PRL 115 (2015) 211101

[2] A.D. Panov et al. (ATIC Collaboration), Bull. Russ. Acad. Sci.: Phys. 73 (2009) 564

[3] K. Abe et al. (BESS Collaboration), Adv. Space Res. (2017), *http://dx.doi.org/10.1016/j.asr.2016.11.004*

[4] Y.S. Yoon et al. (CREAM Collaboration), Astrophys. J. 839 (2017) 1

[5] O. Adriani et al. (PAMELA Collaboration), Science 332 (2011) 69

[6] J.Chang et al (DAMPE Collaboration), arXiv:1706.08453

[7] Y. Yu et al, arXiv:1703.00098

[8] P. Azzarello et al., Nucl. Instrum. Meth. A 831 (2016) 378-384

[9] Z. Zhang et al, Nucl. Instrum. Meth. A 836 (2016) 98

[10] W. Jiang et al., *Determination of the South Atlantic Anomaly from DAMPE data*, POS(ICRC2017)228

[11] S. Agostinelli, et al., Nucl. Instrum. Meth. A 506 (2017) 3

[12] Y. Zhang et al., *PSD performance and charge reconstruction with DAMPE*, POS(ICRC2017)168

[13] S. Vitillo et al., *Measurement of cosmic rays charge with DAMPE Silicon-Tungsten Tracker*, POS(ICRC2017)240

[14] *https://root.cern.ch*

[15] G. D'Agostini, Nucl.Instrum.Meth. A362 (1995) 487-498

[16] M.N. Maziotta, arXiv:0912.1236

[17] F. Loparco, M.N. Maziotta, arXiv:0912.3695